Commun. Theor. Phys. **63** (2015) 625–634 Vol. 63, No. 5, May 1, 2015

Structural and Interaction Properties of Porphyrin Layers — A Quantum Chemical Study

G. Praveena[1,*] and A. Abiram[2]

[1]Department of Physics, PSGR Krishnammal College for Women, Coimbatore 641004, India

[2]Department of Physics, Karunya University, Coimbatore 641114, India

(Received September 4, 2014; revised manuscript received October 16, 2014)

Abstract *This paper is proposed to understand the interaction of porphyrin layers with diatomic molecules interacting at their interior regions by applying ab initio and density functional theory (DFT) methods. We have used NO, CO, and O_2 diatomic molecules to interact with the porphyrin layers. The most common Fe-centered metalloporphyrin structure with tetra-pyrrlic rings having N4 core is chosen for the study. The optimization of Porphyrin-Porphyrin (P_I-P_{II}) and Porphyrin-Diatomic molecule-Porphyrin (P_I-AB-P_{II}) (AB = NO, CO, and O_2) complexes are performed using HF method. In order to understand the planarity and appropriate stacking size of porphyrins and also to infer the separation of diatomic molecules between porphyrin layers the behavior of P_I-AB-P_{II} complexes (where AB = NO, CO, and O_2) are analyzed using structural properties and molecular electrostatic potentials (MEP). The MEPs are calculated using hybrid exchange correlation functional B3PW91 of DFT along with 6-31+G* basis set for the P_I-P_{II} and P_I-AB-P_{II} complexes obtained from HF method.*

PACS numbers: 71.15.-m, 71.15.Mb, 71.15.Nc, 78.55.Hx, 81.07.Pr, 81.07.Nb, 81.16.Dn
Key words: porphyrin, *ab initio*, density functional theory, diatomic molecules, molecular storage

1 Introduction

The self-assembled nanostructures with well-defined shapes and dimensions are of great interest in electronics, photonics, light-energy conversion, and catalytic[1−3] applications. It is well known that because of the vast biological and structural functions, porphyrins are of both scientifically and industrially important systems. In recent years, in addition to various peptide based bionanostructures,[4−7] nanotubular structures of porphyrins have also drawn greater attention among researchers.[8−20] Further, metalloporphyrins are recognized as attractive building blocks of supramolecular assemblies toward the construction of functional materials.[21−24] In a continuing effort of devising nanometer scale structures of porphyrin, several of successful strategies have been developed in recent years.[8−17]

Porphyrin nanostructures such as molecular squares, cages and capsules are sustained by means of metal ion binding auxiliaries[8−16] or by direct perpendicular intercoordination of individual porphyrin units.[17] Furthermore, the molecular building blocks of porphyrin nanostructures are altered in a particular manner to control the functionalities and such design flexibility has attracted the applicability of porphyrin nanostructures in photochemical devices, chlorosomal rods, guest molecule storage, and transport usages.[8,10,19−20,25]

Apart from significant nanostructural functions, metalloporphyrins are also well known compounds of heme-diatomic structure.[26−42] Heme-diatomic complexation is one of the central biological processes which is responsible for the storage and transport of dioxygen by the respiratory proteins like myoglobin and hemoglobin, sensing of NO by soluble guanylate cyclase, a key physiological process in vasodilations, and in the reduction of NO and nitrite in global nitrogen cycle.[26−27] A wide range of experimental studies have provided a significant explanation on the nature of heme-diatomic interactions and the discrimination of heme among the diatomic ligands.[28−33] Exploration of Iron (Fe)-porphyrin complexes with NO, CO and O_2 diatomic molecules has demonstrated the use of Fe-porphyrin-diatomic complexes to understand the heme-diatomics.[34−36] Such studies have resulted in a good description of Fe-diatomic bonding and also provided several important spectroscopic properties on heme-diatomics. Various theoretical studies discussing the discrimination of diatomic molecules by heme were also performed on the Fe-porphyrin-diatomic complexes.[37−39] Subsequently, understanding Fe-NO, Fe-CO and Fe-O_2 porphyrin chemistry in particular in the penta and hexa coordinated Fe-diatomic porphyrin complex has become vital and henceforth widespread efforts were undertaken to elucidate the details of their bonding as well as structural properties.[40−42] A study carried out at PW91/STO-TZP level of theory has reported some of the specific properties like arrangements of diatomic units and described the

*Corresponding author, E-mail: gopalpraveena@gmail.com

© 2015 Chinese Physical Society and IOP Publishing Ltd

local interaction of a distal pocket hydrogen bond donor with heme-bound diatomic complexes in both penta and hexa coordinated states.[41]

Though large number of experimental and theoretical studies on the characterization and interaction of single porphyrin molecule with diatomic molecules are available,[8−25] theoretical work on the molecular sensing and storage properties of their stacked layers are almost absent in the literature. Hence, in this work, we perform a theoretical investigation on the interaction of porphyrin layers with diatomic molecules present at their interior regions applying *ab initio* and density functional theory (DFT) methods. Such a study in turn would provide a detailed understanding on the mechanism of sensing diatomic species by heme and thereby yield an insight into the molecular storage behavior of self assembling porphyrin nanotubular arrays. We have used NO, CO and O_2 diatomic molecules to interact between the porphyrin layers as they reflect ligand-binding properties of proteins uniquely in hemoglobin and myoglobin and are the ubiquitous molecules in biological systems.[26−42] The N_4 core porphyrin structure is found to have easy metal complexing ability[43] than others.[44−45] Hence the most common Fe-centered metalloporphyrin structure with tetra-pyrrlic rings having N4 core is chosen for the study.

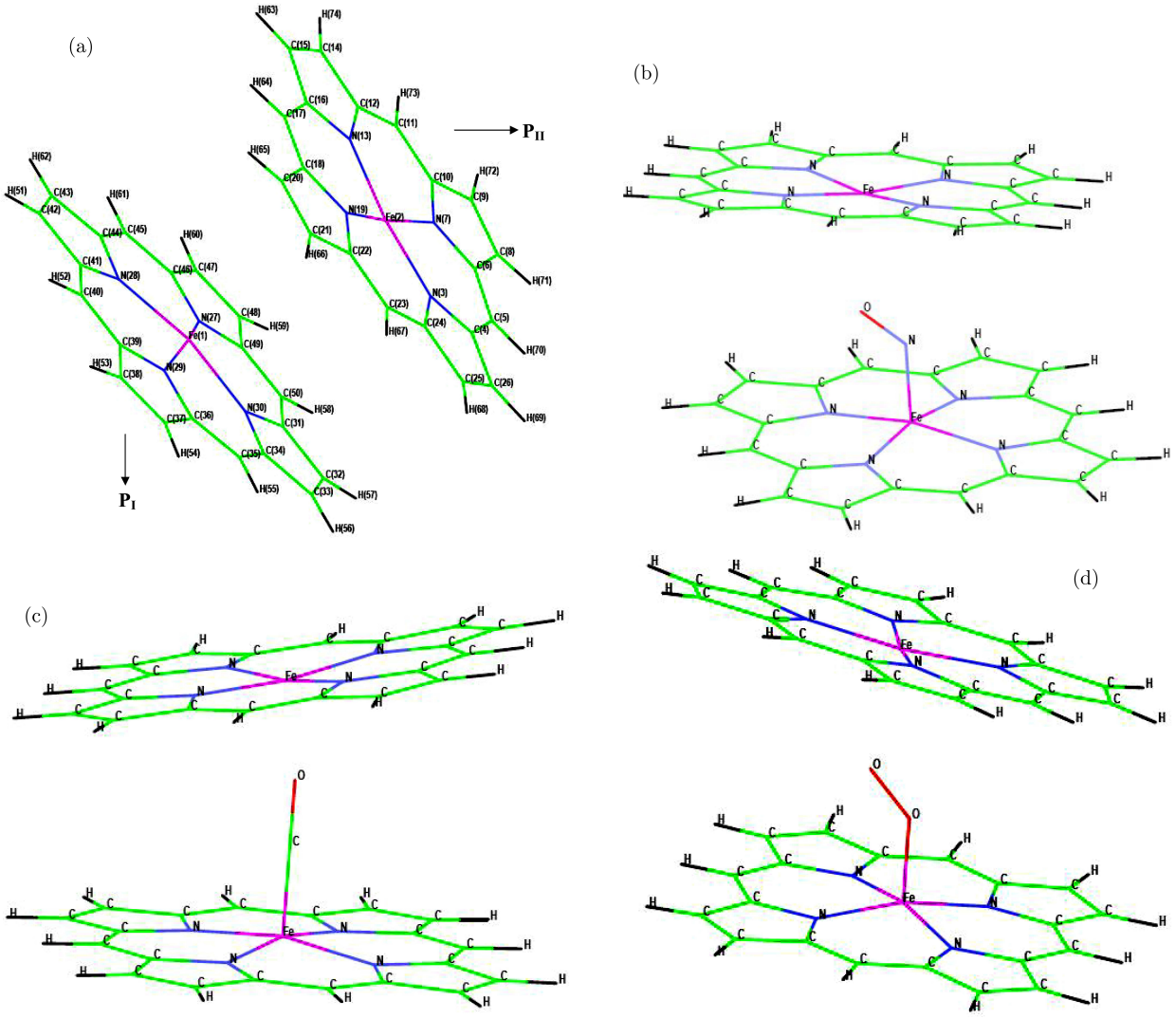

Fig. 1 Structure of (a) P_I-P_{II} (b) P_I-NO-P_{II} (c) P_I-CO-P_{II} and (d) P_I-O_2-P_{II} complexes used for optimizations with (a) showing the numbering scheme used throughout.

The porphyrin-porphyrin layer (denoted as P_I-P_{II}) used for the present study is given in Fig. 1(a). Also the diatomic molecules NO, CO, and O_2 interacting at the interior regions of porphyrin layer used for optimizations are shown in Figs. 1(b), 1(c), and 1(d) (herein after denoted as P_I-AB-P_{II} where AB = NO, CO, and O_2). In order to maintain the appropriate functionalization of porphyrin scaffold, firstly the diatomic molecules

are introduced on to the P_I framework, where diatomic molecules are metalated with Fe1 of P_I. After attaining the penta-coordinated preference, P_{II} framework is then placed above it facing the diatomic molecule in order to ensure a perfectly structured layer rather than a divergent construction. The behavior of P_I-AB-P_{II} complexes is analyzed using structural properties and many body analysis. Also molecular electrostatic potential (MEP) calculation is performed to understand the planarity and appropriate stacking distance of porphyrins, and also to infer the separation of diatomic molecules between porphyrin layers.

2 System Set-Up and Method of Calculation

Because the computational requirements are fewer, HF method is commonly preferred over correlated methods for preliminary structural calculations. Despite the simplified description of electron interactions, the HF method offers reasonable energies, wavefunctions, electron density distributions and other atomic, and molecular properties.[46] The optimizations of P_I-P_{II} and P_I-AB-P_{II} (AB = NO, CO and O_2) complexes are performed using HF method with STO-3G as basis set. Even though HF method is incapable of describing weak van der Waals interactions; the aim here is solely to understand the structural behavior of porphyrin layers upon diatomic enclosures. In order to find the dominant mode of interactions involved in the P_I-P_{II} and P_I-AB-P_{II} complexes the many-body analysis[47] is also carried out at B3PW91/6-31+G*//HF/STO-3G level of theory. The binding energies are divided into two- and three-body systems as in following equations:

$$\Delta^2 E(\mathrm{P_I}\ldots\mathrm{P_{II}}) = E(\mathrm{P_I}\ldots\mathrm{P_{II}}) - E(\mathrm{P_I}) - E(\mathrm{P_{II}})\,, \quad (1)$$

$$\Delta^2 E(\mathrm{P_I}\ldots\mathrm{AB}) = E(\mathrm{P_I}\ldots\mathrm{AB}) - E(\mathrm{P_I}) - E(\mathrm{AB})\,, \quad (2)$$

$$\Delta^2 E(\mathrm{P_{II}}\ldots\mathrm{AB}) = E(\mathrm{P_{II}}\ldots\mathrm{AB}) - E(\mathrm{P_{II}}) - E(\mathrm{AB})\,, \quad (3)$$

$$\Delta^3 E(\mathrm{P_I}\ldots\mathrm{AB}\ldots\mathrm{P_{II}}) = E(\mathrm{P_I}\ldots\mathrm{AB}\ldots\mathrm{P_{II}}) - E(\mathrm{P_I}) - E(\mathrm{AB}) - E(\mathrm{P_{II}})\,, \quad (4)$$

$$\Delta E_{\mathrm{tot}} = \Delta^3 E(\mathrm{P_I} - \mathrm{AB} - \mathrm{P_{II}}) - \Delta^2 E(\mathrm{P_I}\ldots\mathrm{AB}) - \Delta^2 E(\mathrm{P_{II}}\ldots\mathrm{AB}) - \Delta^2 E(\mathrm{P_I}\ldots\mathrm{P_{II}})\,, \quad (5)$$

where Δ^2E, for the pairs $P_I\ldots P_{II}$, $P_I\ldots AB$, and $P_{II}\ldots AB$, are the decomposed two-body binding energies and Δ^3E in all the (P_I-AB-P_{II}) (AB = NO, CO, and O_2) complexes are the three-body binding energies. All the calculations were performed using Gaussian 09 program package.[48] The MEPs are calculated through single point energy calculations using hybrid exchange correlation functional B3PW91 of DFT along with $6-31+G^*$ basis set for the P_I-P_{II} and P_I-AB-P_{II} (AB = NO, CO, and O_2) complexes obtained at HF/STO-3G level.

3 Results and Discussion

3.1 *Structure of P_I-P_{II} and (P_I-AB-P_{II}) (AB = NO, CO, and O_2) Complexes*

As mentioned above, initially the diatomic molecules NO, CO, and O_2 were positioned between the porphyrin layers in such a way that it binds covalently with Fe1 atom of P_I and non-covalently with Fe2 of P_{II} (see Figs. 1(b), 1(c), and 1(d)). But the optimizations of such penta coordinated complexes are resulted in variety of structural deviations, exhibiting interesting features of diatomic molecular interaction in porphyrin layers. Figure 1(a) depicts the atomic labeling convention used. The distance between Fe1 and Fe2 atoms of the respective P_I and P_{II} planes is calculated to understand the stacking distances. The Fe1-Fe2 distance and some of the significant bond lengths such as A-B, Fe-A, Fe-B, and Fe-N in all the complexes are presented in Table 1. In the optimized structure of isolated P_I-P_{II} layer depicted in Fig. 2, the porphyrin planes are found to be separated by a distance of 3.62 Å with considerable deviation in their planarity.

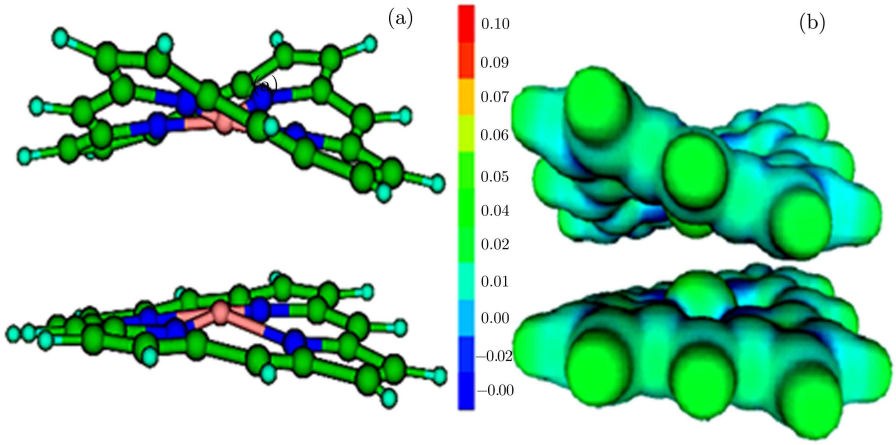

Fig. 2 (Color online) Optimized structure of a) isolated P_I-P_{II} layer and b) its molecular electrostatic potential map. The isosurface value of 0.05 with a range for the MEP of −0.03 to 0.10 a.u. The plots show regions ranging from positive (red) to negative (blue) electrostatic potentials; the values of the electrostatic potentials are indicated in the scale.

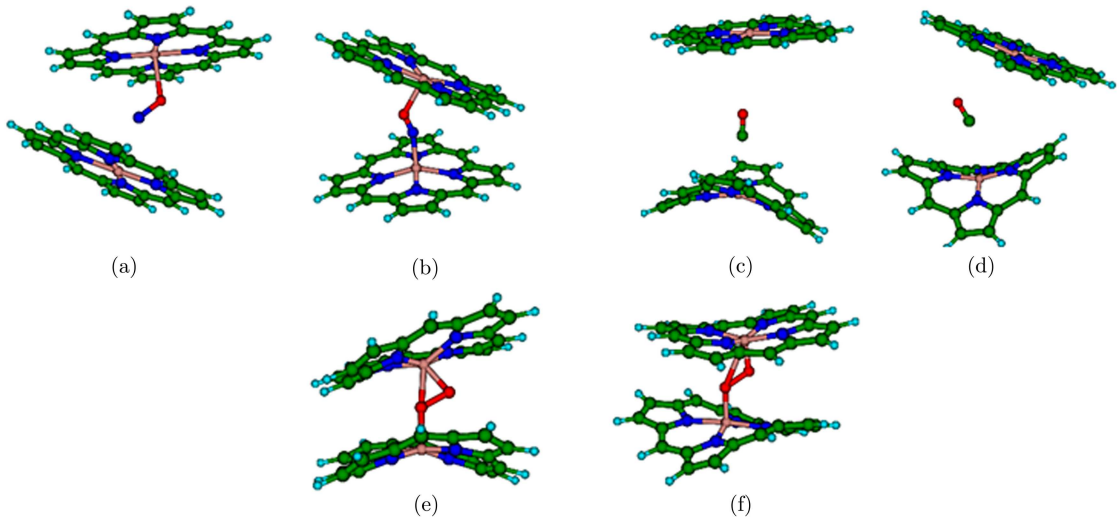

Fig. 3 (Color online) Optimized structures of a) $(P_I\text{-}NO\text{-}P_{II})_1$ b) $(P_I\text{-}NO\text{-}P_{II})_2$ c) $(P_I\text{-}CO\text{-}P_{II})_1$ d) $(P_I\text{-}CO\text{-}P_{II})_2$ e) $(P_I\text{-}O_2\text{-}P_{II})_1$, and f) $(P_I\text{-}O_2\text{-}P_{II})_2$ complexes.

Table 1 Bond lengths A-B, Fe-A, Fe-B, Fe-N and Fe-Fe (in Å) of P(I)-P(II) and P(I)-AB-P(II) (where AB = NO, CO, and O_2) complexes optimized at HF/STO-3G level of theory.

Parameters	P	$(NO)_1$	$(NO)_2$	$(CO)_1$	$(CO)_2$	$(O_2)_1$	$(O_2)_2$
A-B	–	1.324	1.268	1.144	1.145	1.377	1.378
		(1.12)	(1.12)	(1.12)	(1.12)	(1.28)	(1.28)
Fe1-A	–	2.781	1.949	2.994	3.155	1.752	1.665
		(1.71)	(1.71)	(1.77)	(1.77)	(1.75)	(1.75)
Fe1-B	–	3.967	3.142	4.137	4.248	2.683	2.615
Fe2-B	–	2.354	1.999	4.159	3.915	1.587	1.506
Fe2-A	–	3.226	2.886	5.300	4.218	1.842	2.400
Fe1-N30	1.936	1.958	1.968	1.876	1.865	1.929	1.957
		(2.00)	(2.00)	(2.02)	(2.02)	(1.98)	(1.98)
Fe1-N25	2.058	2.185	2.128	1.722	1.725	1.806	1.808
Fe1-N29	1.871	1.969	1.969	1.875	1.866	1.920	1.935
Fe2-N27	2.056	1.911	2.117	1.721	1.720	1.794	1.800
Fe2-N3	1.731	1.961	2.205	2.036	1.874	1.959	1.903
Fe2-N19	1.906	1.921	1.986	1.886	2.056	1.896	1.959
Fe2-N13	1.735	1.969	1.941	2.031	1.934	2.003	1.990
Fe2-N7	1.905	2.179	1.997	1.935	2.056	2.046	1.962
Fe1- Fe2	3.621	5.992	4.791	8.294	6.769	3.589	3.961

Note: (NO)1, (NO)2, (CO)1, (CO)2, (O2)1 and (O2)2 denote (PI-NO-PII)1, (PI-NO-PII)2, (PI-COPII)1, (PI-CO-PII)2, (PI-O2-PII)1 and (PI-O2-PII)2 complexes. The values given in the parentheses are the experimentally obtained geometrical bond lengths of heme diatomic models.[58−61]

During optimization of the initially generated P_I-NO-P_{II} structure (see Fig. 1(b)), the O atom of NO binds to Fe2 of P_{II}, whereas its nitrogen atom is non-bonded to Fe1 of P_I as seen in Fig. 3(a). Comparing the distance of Fe atoms from the respective diatomic sites, Fe2-O distance (2.354 Å) is found to be smaller than Fe1-N distance (2.781 Å). Furthermore, the separation of porphyrin layers in the optimized NO complex is found to be 6.0 Å. When P_I-CO-P_{II} complex (Fig. 1(c)) is optimized, it takes up a structure where CO is found to be cleft away from Fe1 and interacts non-covalently between P_I and P_{II} layers (see Fig. 3(c)). Further, porphyrin units in the optimized CO complex are found to be separated by a larger distance of about 8.0 Å. After optimizing the P_I-O_2-P_{II} structure (Fig. 1(d)), the stacking distance of P_I and P_{II} planes in the resultant O_2 complex (Fig. 3(e)) is found to be 3.6 Å, which is very much similar to that of the isolated P_I-P_{II} structure (Fig. 2). The strong binding affinity of O_2 molecule towards Fe1 and Fe2 might be the cause for reduction in the stacking distance of O_2 complex. Herein after we will represent the three optimized NO, CO, and O_2 complexes using the subscript 1 as, $(P_I\text{-}NO\text{-}P_{II})_1$, $(P_I\text{-}CO\text{-}P_{II})_1$, and $(P_I\text{-}O_2\text{-}P_{II})_1$ respectively.

Table 2 Energetical parameters: Total energy (in hartrees), relative energy of $(P_I\text{-AB-}P_{II})_{1\&2}$ complexes (in kcal/mol) and the many body analysis: two-body (Δ^2E), three-body (Δ^3E) and the total interaction energies (ΔE_{tot}) (in kcal/mol) of $P_I\text{-}P_{II}$ and $(P_I\text{-AB-}P_{II})_{1\&2}$ complexes obtained at B3PW91/6-31+G*//HF/STO-3G level of theory.

System	T.E	R.E	Δ^3E	$\Delta^2E_{(PI\ldots PII)}$	$\Delta^2E_{(PII\ldots AB)}$	$\Delta^2E_{(PI\ldots AB)}$	ΔE_{tot}
$P_I\text{-}P_{II}$	−4503.14	–	–	–	–	–	–
$(P_I\text{-NO-}P_{II})_1$	−4633.12	0.0	−74.34	1.30	−23.73	−26.58	−25.3
$(P_I\text{-NO-}P_{II})_2$	−4633.09	18.51	−61.14	−1.62	−41.91	−23.52	5.94
$(P_I\text{-CO-}P_{II})_1$	−4616.41	0.0	0.14	−1.43	6.77	−3.57	−1.62
$(P_I\text{-CO-}P_{II})_2$	−4616.41	0.37	−3.38	−6.23	−0.16	1.33	1.68
$(P_I\text{-}O_2\text{-}P_{II})_1$	−4653.44	30.37	−70.60	0.35	−76.51	−65.66	71.22
$(P_I\text{-}O_2\text{-}P_{II})_2$	−4653.48	0.0	−110.86	30.75	−75.33	−67.08	0.80

Table 3 Bond angles: ∠N-Fe-N, ∠Fe1-A-B, ∠Fe2-B-A, ∠Fe1-A-B-Fe2 and angles ∠T1 and ∠T2 describing the planarity of porphyrin planes (in degrees) of $P_I\text{-}P_{II}$ and $(P_I\text{-AB-}P_{II})_{1\&2}$ complexes optimized at HF/STO-3G level of theory.

Parameters	P	$(NO)_1$	$(NO)_2$	$(CO)_1$	$(CO)_2$	$(O_2)_1$	$(O_2)_2$
∠N30-Fe1-N29	170.2	172.3	154.3	161.7	157.1	174.2	175.2
∠N25-Fe1-N27	159.4	178.9	168.3	155.0	158.5	155.2	151.6
∠N3-Fe2-N13	153.8	172.4	169.3	180.0	175.3	146.3	158.0
∠N19-Fe2-N7	168.4	179.4	163.8	179.8	170.9	156.9	160.2
∠Fe1-A-B	–	148.2	154.7	177.0	159.9	117.6	118.2
		(149.0)	(149.0)	(179.0)	(179.0)	(131.0)	(131.0)
∠Fe2-B-A	–	120.0	122.6	175.7	97.4	76.5	112.6
∠Fe1-A-B-Fe2	–	173.5	−156.7	−147.1	171.1	177.3	179.1
∠T1	162.1	178.4	175.6	147.2	149.6	152.7	149.8
∠T2	159.4	179.6	170.0	179.7	173.1	173.3	166.7

Note: The values given in the parentheses are the experimentally obtained geometrical bond lengths of heme diatomic models.[58−61]

The stacking distances of the order of 6.0 and 8.0 Å are observed for $(P_I\text{-NO-}P_{II})_1$ and $(P_I\text{-CO-}P_{II})_1$ complexes. Hence in order to get more information on the influence of non-bonded porphyrin planes over diatomic molecule, we have tried to optimize the NO and CO structures by reducing their Fe1-Fe2 distance. Also, due to the shorter stacking distance in $(P_I\text{-}O_2\text{-}P_{II})_1$ complex, we have made an attempt to optimize the O_2 complex by increasing its Fe1-Fe2 distance. Such optimizations might be useful in exploring the separation of molecules that are sandwiched between porphyrin layers. For convenience, such structures are denoted with subscript 2 as, $(P_I\text{-NO-}P_{II})_2$, $(P_I\text{-CO-}P_{II})_2$, and $(P_I\text{-}O_2\text{-}P_{II})_2$ respectively, and are presented in Figs. 3(b), 3(d), and 3(f). The relative energies of the respective $(P_I\text{-AB-}P_{II})_{1\&2}$ (AB = NO, CO, and O_2) complexes are given in Table 2. It is interesting to see the dependence of trend in relative energy on the stacking distances. The complexes with larger stacking distance are relatively high in negative energy than the complexes with shorter stacking distance. The complexes $(P_I\text{-NO-}P_{II})_1$, $(P_I\text{-CO-}P_{II})_1$, and $(P_I\text{-}O_2\text{-}P_{II})_2$ with quite larger in stacking distances of 6.0, 8.3, and 4.0 Å respectively are found to be more stable than $(P_I\text{-NO-}P_{II})_2$, $(P_I\text{-CO-}P_{II})_2$, and $(P_I\text{-}O_2\text{-}P_{II})_1$ complexes possessing slightly shorter Fe1-Fe2 distances.

Further the geometrical parameters of the isolated $P_I\text{-}P_{II}$ and $(P_I\text{-AB-}P_{II})_{1\&2}$ complexes are compared to understand the structural discrimination. The variation of stacking distances follows the order as: $(P_I\text{-CO-}P_{II})_{1\&2}$ (with Fe1-Fe2 ≈ 7–8 Å) > $(P_I\text{-NO-}P_{II})_{1\&2}$ (with Fe1-Fe2 ≈ 5–6 Å) > $(P_I\text{-}O_2\text{-}P_{II})_{1\&2}$ (with Fe1-Fe2 ≈ 3.6–4 Å). The differences in stacking distance are clearly due to the electronic occupation of diatomic molecules available for the interaction with Fe atoms of porphyrin planes. It is seen that for $(P_I\text{-AB-}P_{II})_{1\&2}$ (where AB = NO and CO) complexes, the projection of A-B bond lies in phase with one of the Fe-N bonds of upper porphyrin P_{II} plane. Whereas in the case of $(P_I\text{-}O_2\text{-}P_{II})_{1\&2}$ complexes, the projection of O_2 bond lies along the bisection of one of the N-Fe-N angles of P_{II}. Similar effect is already observed in the complexation of single porphyrin layer with diatomic molecules[40] where A-B bond projects along the N-Fe-N angles of porphyrin surface. Further, our results for Fe-N geometrical parameters compare well with the previous experimental values[49−52] (see Table 1), except few of Fe-N bonds which vary by about ±0.3 Å. The significant variations in Fe-N bond lengths of $(P_I\text{-AB-}P_{II})_{1\&2}$ complexes from that of the isolated $P_I\text{-}P_{II}$ structure are noted,

which is clearly due to the effect of diatomic molecules on porphyrin planes. Comparison between the experimental data of Fe-porphyrin diatomic complexes[49−52] with our values shows that the computed A-B distances are larger by about 0.02–0.2 Å. Of all the complexes, a larger deviation in A-B is noted for $(P_I\text{-AB-}P_{II})_{1\&2}$ (AB = NO and O_2) complexes. Such elongation effect can easily be rationalized on the basis of the influence of both P_I and P_{II} planes over diatomic molecules. Since stacking distances are quite longer (7–8 Å) in $(P_I\text{-CO-}P_{II})_{1\&2}$ complexes, the influence of P_I and P_{II} is less and hence CO undergoes less distortion than NO and O_2 in the respective complexes.

Table 3 lists some of the key geometrical bond angle parameters for $P_I\text{-}P_{II}$, $(P_I\text{-AB-}P_{II})_{1\&2}$ complexes. As seen earlier, the binding feature of metal-diatomic molecule, ∠M-A-B (where M is the metal), is effectively important in understanding the discrimination of diatomic molecules by heme-proteins.[52] The NO, CO, and O_2 bound protein and heme derivatives were found to exhibit a bent M-A-B conformation,[49,53−58] wherein M-CO unit also shows linear geometry.[37,50,59−62] It is worth mentioning that the bending and linear conformational aspects of M-A-B units were implicated in probing the structural basis of binding and discrimination of diatomic molecule when bind to hemes.[41,60] The Fe-A-B geometrical angles of $(P_I\text{-AB-}P_{II})_{1\&2}$ (AB = NO, CO, and O_2) complexes are calculated and listed in Table 3. Except for $(P_I\text{-CO-}P_{II})_1$ complex, the Fe1-A-B angles of all the remaining structures occur in bent conformation, which coincides with the observed experimental results for diatomic molecule bound penta-coordinated heme complexes.[49−52] The differences in Fe1-CO geometry of $(P_I\text{-CO-}P_{II})_{1\&2}$ are easily visualized in Figs. 3(c) and 3(d). It has often been invoked that the bending of Fe-CO angle is responsible for the weakening of CO binding to heme in myoglobin.[53−54] In the $(P_I\text{-CO-}P_{II})_2$ complex with bent Fe1-CO geometry, the plane of P_{II} slides over P_I. Whereas in $(P_I\text{-CO-}P_{II})_1$ complex with linear Fe1-CO conformation, the P_{II} plane is perfectly stacked above P_I without sliding. This discrimination in the structural arrangement of porphyrin planes could easily be rationalized in terms of the effect of diatomic molecule over the plane. In $(P_I\text{-CO-}P_{II})_2$ with bent Fe1-CO geometry, the precise projection of CO bond over one of the Fe-N bonds of P_{II} may be the cause for P_{II} plane to slide over the P_I. The influence of P_{II} plane is reflected in the Fe-NO value (154.7° of $(P_I\text{-NO-}P_{II})_2$ complex, which is longer by ≈ 5° than the experimental one. Further, the reduction in Fe-O_2 angles by about ≈ 14° from the experimental value is observed for $(P_I\text{-}O_2\text{-}P_{II})_{1\&2}$ complexes. It is really exciting to see the sliding of porphyrin planes one above the other when diatomic molecules are inserted. Such an arrangement of porphyrin planes which are not positioned directly one on the top of the other is experimentally observed during the self-assembly of diacid TPPS.[25]

Overall, it is observed that the geometrical parameters of $(P_I\text{-AB-}P_{II})_{1\&2}$ (AB = NO, CO, and O_2) complexes coincide well with the experimental values of penta-coordinated heme-diatomic models. Further, sensible changes in Fe-AB and A-B bond distances obviously show the effect of porphyrin planes over the interacting diatomic molecules.

3.2 *Planarity of Porphyrin Planes in P_I-P_{II} and $(P_I\text{-}AB\text{-}P_{II})_{1\&2}$ Complexes*

In order to understand the planarity of porphyrin planes upon diatomic enclosure the planar angles T1 and T2 are calculated and tabulated in Table 3. The parameters T1 and T2 are obtained by choosing atoms randomly along the respective P_I and P_{II} planes. It is seen from Fig. 2 that isolated $P_I\text{-}P_{II}$ structure takes up a geometry in which Fe2 atom moves out-of-plane and inwards with planarity of P_{II} being disturbed to an angle of T2 = 159.4° away from the normal 180° plane. The plane of P_I of $P_I\text{-}P_{II}$ structure is also found to be distorted from its planarity with T1 value of 162.1°. The planar angles of $(P_I\text{-NO-}P_{II})_1$ structure with T1 = 178.5° and T2 = 179.6° depicts that the porphyrin planes maintain the normal planar structure even after NO interaction. But the porphyrin planes in all other complexes are considerably modified and found to have distorted curved edges (see Fig. 3). As a result, P_I porphyrin core in $(P_I\text{-AB-}P_{II})_{1\&2}$ (AB = CO and O_2) complexes is found to be arched with the distortion of −22.0° to −33.0° from normal plane. Similar distortions were previously noted in diatomic molecules interacted porphyrin structure with Fe in five fold coordination geometry.[40] Furthermore, except for $(P_I\text{-NO-}P_{II})_1$ complex, ∠N-Fe-N of all other complexes also reflect distortion in their respective porphyrin planes (from 146.0° to 168.0° approximately). In general, despite of significant changes in the planarity of P_I and P_{II} planes, the rigidity in stacking of porphyrin layers upon diatomic insertion shows the sturdy nature of porphyrin nanostructures for molecular storage applications.

3.3 *Many-Body Interaction Energy Analysis*

It is very well documented that HF theory mainly due to the absence of electron correlation could not realistically be used to compute quantities related to the absolute energies and most importantly it is incapable of describing weak van der Waals interactions. Even if one approaches the HF limit, the intrinsic error in such quantities could be very large. Hence in order to compute energetical parameters such as relative and interaction energies, single point calculation based on DFT method, which allows us

to rapidly estimate the effect of electron correlation is carried out. The BSSE corrected interaction energy of P_I-P_{II} structure and the many-body interaction energies of (P_I-AB-P_{II})$_{1\&2}$ complexes that are calculated at B3PW91/6−31+G*//HF-STO-3G level of theory are tabulated in Table 2. We have carried out the calculations of two-body interactions, Δ^2E, for the pairs $P_I \ldots P_{II}$, $P_I \ldots AB$ and $P_{II} \ldots AB$ and three-body interactions, Δ^3E in all the (P_I-AB-P_{II})$_{1\&2}$ (AB = NO, CO, and O_2) complexes using Eqs. (1)–(5). In the previous theoretical study,[40] the interaction energy of Fe-diatomic penta coordinated porphyrin complex increases as NO (−35.0 kcal/mol) > CO (−26.0 kcal/mol)> O_2 (−9.0 kcal/mol) respectively. In contrast, the order of two-body interactions Δ^2E($P_I \ldots AB$) and Δ^2E ($P_{II} \ldots AB$) of (P_I-AB-P_{II})$_{1\&2}$ complexes vary noticeably from the previous report.[40] In the present case, the two body interaction energies Δ^2E($P_I \ldots AB$) and Δ^2E($P_{II} \ldots AB$) increasing in the order as: O_2 > NO > CO clearly show the dependence of stacking distances and geometric location of the diatomic molecules. The trend in two-body interactions of all complexes is reflected in the geometric arrangement of porphyrin planes with diatomic molecules. On comparison, it is noted that Δ^2E of (P_I-NO-P_{II})$_2$ complex is much greater in negative energy than (P_I-NO-P_{II})$_1$, which in turn might be due to the shorter geometrical distances in (P_I-NO-P_{II})$_2$ complex (Table 1). Similar dependence of the interaction energies over geometric location is also noted for the remaining complexes.

Among the complexes, $P_{II} \ldots O_2$ pair of (P_I-O_2-P_{II})$_1$ is found to have the most attractive two-body interaction (−76.51 kcal/mol), while $P_{II} \ldots CO$ of (P_I-CO-P_{II})$_1$ possess the repulsive interaction (6.77 kcal/mol) as the result of larger stacking distances. Except $P_I \ldots P_{II}$, the calculated two-body interaction energies of $P_I \ldots AB$ and $P_{II} \ldots AB$ pairs are found to be attractive in (P_I-O_2-P_{II})$_{1\&2}$ and (P_I-NO-P_{II})$_{1\&2}$ complexes. Except for (P_I-CO-P_{II})$_{1\&2}$ complex, the three body interaction energies ($\Delta^3 E$) of all complexes are found to be attractive and larger, wherein the highest contribution of three body interaction is found for (P_I-O_2-P_{II})$_2$ complex (−110.86 kcal/mol). Apart from (P_I-NO-P_{II})$_1$ and (P_I-CO-P_{II})$_1$ complexes, the total interaction energies (ΔE_{tot}) of all the remaining complexes are found to be repulsive, confirming the major contribution of two-body interactions.

Overall results indicate that except for (P_I-CO-P_{II})$_{1\&2}$, the two- and three- body interactions of the remaining complexes are attractive in nature. In general, the considerable three- and two-body interaction energies of (P_I-AB-P_{II})$_{1\&2}$ (AB = NO, CO, and O_2) complexes clearly shows the possibility of diatomic intercalation in porphyrin structures.

3.4 *Molecular Electrostatic Potential*

From the structural propensities, it is observed that during the interaction of NO, CO, and O_2 diatomic molecules, the stacking distances of P_I and P_{II} planes differ from one another. The NO and O_2 diatomic molecules when placed between the porphyrin layers, involve in bonding with Fe centers, whereas CO molecule interacted PI and PII layers are found to be separated by a larger distance of the order of 7.0 Å and 8.0 Å respectively. Such discrimination in the intercalation of diatomic molecules between porphyrin layers could be understood in-depth through MEP as it is found to be one of the important tools for rationalizing the interaction between guest compound with that of any macromolecular target.[63−64] Hence we have mapped electrostatic potential onto the electron density to understand the interacting properties of porphyrin layers in the presence of NO, CO, and O_2 molecules.

The MEP maps of P_I-P_{II} and (P_I-AB-P_{II})$_{1\&2}$ (AB = NO, CO, and O_2) complexes obtained at B3PW91/6-31+G*//HF-STO-3G level of theory are shown in Figs. 2 and 4. In the isolated P_I-P_{II} structure (Fig. 2), the minimum potential regions at nitrogen atomic sites are significantly higher than that at carbon sites. The representation of MEP maps for (P_I-AB-P_{II})$_{1\&2}$ (AB = NO, CO, and O_2) complexes is visually more comprehensible (see in Fig. 4) and gives quite straightforward information on the atomic sties of P_I and P_{II} that are able to interact with the diatomic molecules. The blue regions are more negative electron density sites and it decreases through green to red regions. As seen earlier, in (P_I-NO-P_{II})$_1$ complex, instead of nitrogen atom (N), oxygen atom (O) of NO is found to bind strongly with the Fe of P_{II}. This could easily be understood from the structural effect, which shows shorter value for Fe2-O distance (2.35 Å) than Fe1-N distance (2.78 Å) (see Table 1).

However, the MEP map of (P_I-NO-P_{II})$_1$ shows that though N atom of NO seems to be non-bonded to P_I structure, it contributes little amount of its electron density to Fe1 exhibiting the presence of weak interaction. Further, looking at the molecular electrostatic potential maps of both (P_I-NO-P_{II})$_{1\&2}$ complexes, it is clear that N and O atoms of NO diatomic molecule shares somewhat equal probability in binding with Fe atoms of the respective porphyrins. During the intercalation of diatomic molecules between porphyrin structures, sliding of planes one above the other is noted in few complexes. As already observed, the exact projection of N-O bond over Fe-N bonds causes the O atom to face the N atom of P_{II} plane. This is clearly seen from the MEP of (P_I-NO-P_{II})$_2$ complex wherein more negative electron density (O site) of NO faces the more negative electron density (N region) of P_{II}. Due to this, a

repulsive effect may be induced at the inner surface of P_{II} leading to its inclination on the other side.

In $(P_I\text{-}CO\text{-}P_{II})_{1\&2}$ complexes, MEP clearly discriminates the perfect linear and bent geometry of Fe1-CO bonds. It indicates that as C is less electronegative than O atom, the electron density of O is more clouded towards C atom for CO bonding. Hence, because of this effect in $(P_I\text{-}CO\text{-}P_{II})_1$ complex, though oxygen atom perfectly faces P_{II}, it does not attract its Fe2 atom. In the case of $(P_I\text{-}CO\text{-}P_{II})_2$ complex, due to the bent Fe1-CO geometry and precise projection of CO bond over one of the Fe-N bonds of P_{II}, the negative electron density region of O sees the electron rich N site of P_{II} resulting in repulsion and thereby tilting its plane on to the P_I surface. Comparing the stacking distances of all the complexes, the $(P_I\text{-}O_2\text{-}P_{II})_{1\&2}$ complex is found to have shorter Fe1-Fe2 distances of the order 3.6 and 4.0 Å respectively. The MEP of $(P_I\text{-}O_2\text{-}P_{II})_{1\&2}$ complexes reveals that the more negative electron rich O sites strongly attract the electron deficient Fe atomic sties of both the P_I and P_{II} planes with equal probability. Furthermore, as the O_2 bonds project on to the bisecting region of N-Fe-N angles of P_{II} plane, the sliding of respective porphyrin plane over P_I is not observed in the $(P_I\text{-}O_2\text{-}P_{II})_{1\&2}$ complexes. In general, molecular electrostatic potential maps of $(P_I\text{-}AB\text{-}P_{II})_{1\&2}$ (AB = NO, CO, and O_2) complexes effectively illustrate the discrimination in stacking of diatomic molecules between porphyrin layers and the sliding behavior of porphyrin plane one above the other.

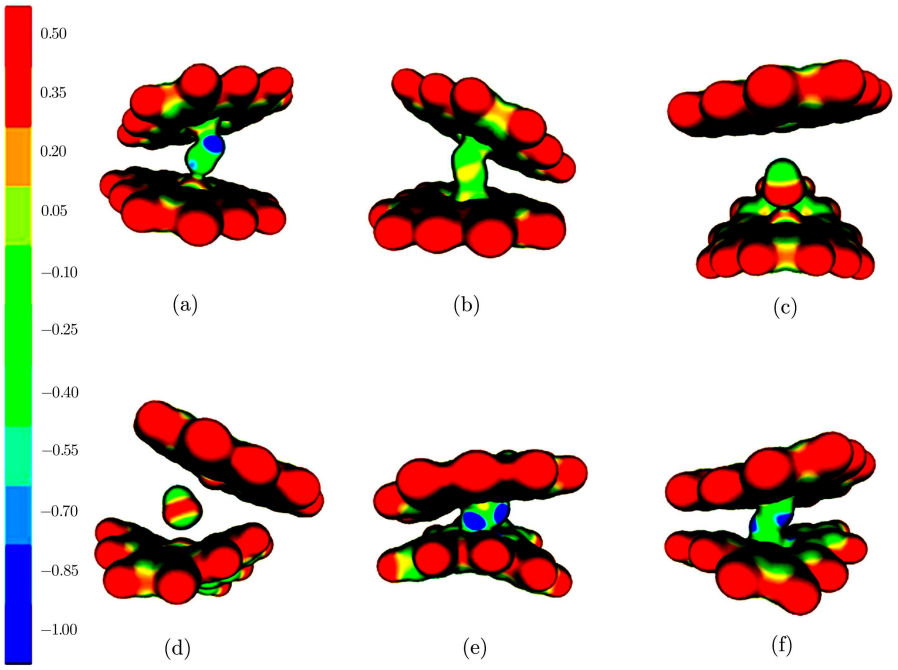

Fig. 4 (Color online) Molecular electrostatic potential maps of a) $(P_I\text{-}NO\text{-}P_{II})_1$, b) $(P_I\text{-}NO\text{-}P_{II})_2$, c) $(P_I\text{-}CO\text{-}P_{II})_1$, d) $(P_I\text{-}CO\text{-}P_{II})_2$, e) $(P_I\text{-}O_2\text{-}P_{II})_1$ and f) $(P_I\text{-}O_2\text{-}P_{II})_2$ complexes. The isosurface value of 0.05 with a range for the MEP of −1.0 to 0.5 a.u. is used. The plots show regions ranging from positive (red) to negative (blue) electrostatic potentials; the values of the electrostatic potentials are indicated in the scale.

4 Conclusion

Analysis of the structural and molecular interacting properties of stacked porphyrin layers is carried out using quantum chemical calculations. The diatomic molecules NO, CO, and O_2 are placed at the interior regions of porphyrin layers and the influence of second porphyrin plane over the diatomic molecule interacted porphyrin structure is studied by varying the stacking distances. The stacking distance of porphyrin planes varies in the order as: $(P_I\text{-}CO\text{-}P_{II})_{1\&2} > (P_I\text{-}NO\text{-}P_{II})_{1\&2} > (P_I\text{-}O_2\text{-}P_{II})_{1\&2}$ respectively. The diatomic molecules NO and O_2 are found to interact with Fe atoms, whereas in the presence of CO molecule the porphyrin planes are separated at larger distances. The effect of porphyrin planes on the geometrical parameters is observed. The geometrical angles Fe-AB of $(P_I\text{-}AB\text{-}P_{II})_{1\&2}$ coincides well with the experimental values of heme-diatomic models. Almost all the two- and three- body interactions of the complexes are found to be attractive in nature. The MEP map effectively describes the discrimination in stacking of porphyrin layers upon the inclusion of diatomic molecules and also gives insight into the influence of atomic sites that are responsible for the sliding of porphyrin planes. Except for deviation in the planarity, the sturdy nature of porphyrin layers and their

discrimination in stacking towards diatomic molecules exhibit their readiness for the sensing of guest molecules. This study on the structure and interaction of diatomic molecules between porphyrin layers would have some potency in the separation of molecules using porphyrin nanotubes, where porphyrin layers are the building blocks of those extended structures. Furthermore, as self assembled porphyrin nanotubes are the promising future biosensors that could show rapid and high sensitivity to chemical compounds, the attractive nature of many body interactions along with the discrimination in the stacking of porphyrin layers in the present study exhibit appropriate patterns for molecular confinement suggesting their potential utilization towards molecular storage and chemical sensor applications.

Acknowledgments

Author G. Praveena is thankful to the Science and Engineering Research Board (SERB), India for awarding the fast track project (Project No: SB/FTP/PS-096/2013).

References

[1] G.M. Whitesides, J.P. Mathias, and C.T. Seto, Science **254** (1991) 1312.

[2] K.E. Martin, Z. Wang, T. Busani, *et al.*, J. Am. Chem. Soc. **132** (2010) 8194.

[3] Y. Tian, C.M. Beavers, T. Busani, *et al.*, Nanoscale **4** (2012) 1695.

[4] M.R. Ghadiri, J.R. Granja, R.A. Milligan, D.E. McRee, and N. Khazanovich, Nature (London) **366** (1993) 324.

[5] D. Seebach, J.L. Mathews, A. Meden, T. Wessels, C. Baerlocher, and L.B. McCusker, Helv. Chim. Acta. **80** (1997) 173.

[6] S. Kubik and R. Goddard, J. Org. Chem. **64** (1999) 9475.

[7] M. Amorin, L. Castedo, and J.R. Granja, J. Am. Chem. Soc. **125** (2003) 2844.

[8] N. Fujita, K. Biradha, M. Fujita, S. Sakamoto, and K. Yamaguchi, Angew. Chem. Int. Ed. **40** (2001) 1718.

[9] E. Iengo, E. Sangrando, R. Minatel, and E. Alessio, J. Am. Chem. Soc. **124** (2002) 1003.

[10] P.H. Dinolfo and J.T. Hupp, Chem. Mater. **13** (2001) 3113.

[11] C.M. Drain, F. Nifiatis, A. Vasenko, and J. Batteas, Angew. Chem. Int. Ed. **37** (1998) 2344.

[12] J. Fan, J.A. Whiteford, B. Olenyuk, M.D. Levin, P.J. Stang, and E.B. Fleischer, J. Am. Chem. Soc. **121** (1999) 2741.

[13] K. Ogawa, T. Zhang, K. Yoshihara, and Y. Kobuke, J. Am. Chem. Soc. **124** (2002) 22.

[14] U. Michelsen and C.A. Hunter, Angew. Chem. Int. Ed. **39** (2000) 764.

[15] R. Franco, J.L. Jacobsen, H. Wang, *et al.*, Phys. Chem. Chem. Phys. **12** (2010) 4072.

[16] T. Ishizuka, M. Sankar, Y. Yamada, S. Fukuzumi, and T. Kojima, Chem. Commun. **48** (2012) 6481.

[17] K. Fukushima, K. Funatsu, A. Ichimura, *et al.*, Inorg. Chem. **42** (2003) 3187.

[18] Z. Wang, C.J. Medforth, and J.A. Shelnutt, J. Am. Chem. Soc. **126** (2004) 15954.

[19] M.H. Keefe, J.L. O'Donnell, R.C. Bailey, S.T. Nguyen, and J.T. Hupp, Adv. Mater. **15** (2003) 1936.

[20] Z. Wang, C.J. Medforth, and J.A. Shelnutt, J. Am. Chem. Soc. **126** (2004) 16720.

[21] S. Okada and H. Segawa, J. Am. Chem. Soc. **125** (2003) 2792.

[22] B.L. Iverson, K. Shreder, V. Kral, P. Sansom, V. Lynch, and J.L. Sessler, J. Am. Chem. Soc. **118** (1996) 1608.

[23] J.S. Hu, Y.G. Guo, H.P. Liang, L.J. Wan, and L. Jiang, J. Am. Chem. Soc. **127** (2005) 17090.

[24] T. Hasobe, S. Fukuzumi, and P.V. Kamat, J. Am. Chem. Soc. **127** (2005) 11884.

[25] A.D. Schwab, D.E. Smith, C.S. Rich, E.R. Young, W.F. Smith, and J.C. de Paula, J. Phys. Chem. B **107** (2003) 11339.

[26] L.J. Ignarro, *Nitric Oxide — Biology and Pathobiology,* ed., L. Ignarro, Academic Press, San Diego (2000) pp. 3–19.

[27] N. Toda and T. Okamura, Pharmacol. Rev. **55** (2003) 271.

[28] J.S. Olson and G.N. Philips, J. Biol. Inorg. Chem. **2** (1997) 544.

[29] E.M. Boon and M.A. Marletta, J. Inorg. Biochem. **99** (2005) 892.

[30] D.S. Karow, D. Pan, R. Tran, P. Pellicena, A. Persely, R.A. Mathies, and M.A. Marletta, Biochemistry **43** (2004) 10203.

[31] P. Nioche, V. Berka, J. Vipond, N. Minton, A.L. Tsai, and C.S. Raman, Science **306** (2004) 1550.

[32] P. Pellicena, D.S. Karow, E.M. Boon, M.A. Marletta, and J. Kuriyan, Proc. Natl. Acad. Sci. **101** (2004) 12854.

[33] E.M. Boon, S.H. Huang, and M.A. Marletta, Nature. Chem. Biol. **1** (2005) 53.

[34] G.R.A. Wyllie and W.R. Scheidt, Chem. Rev. **102** (2002) 1067.

[35] R. Hoffmann, M.M.L. Chen, and D.L. Thorn, Inorg. Chem. **16** (1977) 503.

[36] A. Waleh, N. Ho, L. Chantranupong, and G.H. Loew, J. Am. Chem. Soc. **111** (1989) 2767.

[37] A. Ghosh and D.F. Bocain, J. Phys. Chem. **100** (1996) 6363.

[38] T.G. Spiro and P.M. Kozlowski, J. Am. Chem. Soc. **120** (1998) 4524.

[39] I. Papai, A. Stirling, J. Mink, and K. Nakamoto, Chem. Phys. Lett. **287** (1998) 531.

[40] C. Rovira, K. Kunc, J. Hutter, P. Ballone, and M. Parrinello, Int. J. Quant. Chem. **69** (1998) 31.

[41] E. Tangen, A. Svadberg, and A. Ghosh, Inorg. Chem. **44** (2005) 7802.

[42] E. Sigfridsson and U.J. Ryde, Inorg. Biochem. **91** (2002) 101.

[43] H.J. Nilsen and A. Ghosh, Acta. Chem. Scand. **52** (1998) 827.

[44] J.L. Sessler and S.J. Weghorn, *Expanded, Contracted & Isomeric Porphyrins*, Pergamon/Elsevier, Wiltshire, UK (1997).

[45] E.J. Vogel, Heterocycl. Chem. **33** (1996) 1461.

[46] D. Cremer, *Møller-Plesset Perturbation Theory: Encylcopedia of Computational Chemistry,* ed., von Ragué Schleyer P, Wiley, Chichester **3** (1998) pp. 1706-1734.

[47] S.S. Xantheas, J. Chem. Phys. **100** (1994) 7523.

[48] M.J. Frisch, G.W. Trucks, and J.A. Pople, Gaussian, Inc., Pittsburgh PA (2003).

[49] G.B. Jameson, G.A. Rodley, W.T. Robinson, R.R. Gagne, C.A. Reed, and J.P. Collman, Inorg. Chem. **17** (1978) 850.

[50] S.M. Peng and J.A. Ibers, J. Am. Chem. Soc. **98** (1976) 8032.

[51] W.R. Scheidt and M.E. Frise, J. Am. Chem. Soc. **97** (1975)17.

[52] W.R. Scheidt and P.L. Piciulo, J. Am. Chem. Soc. **98** (1976) 1913.

[53] J.P. Collman, J.I. Brauman, T.R. Halbert, K.R. Suslick, Proc. Natl. Acad. Sci. **73** (1976) 3333.

[54] W.S. Caughey, Ann NY Acad. Sci. **174** (1970) 148.

[55] J. Kuriyan, S. Wilz, M. Karplus, and G.A. Petsko, J. Mol. Biol. **192** (1986) 133.

[56] S.E.V. Phillips, J. Mol. Biol. **142** (1980) 531.

[57] J.P. Collman, R.R. Gagne, C.A. Reed, W.T. Robinsin, and G.A. Rodley, Proc. Natl. Acad. Sci. **71** (1974) 1326.

[58] G.B. Jameson, F.S. Molinaro, J.A. Ibers, J.P. Collman, J.I. Brauman, E. Rose, and K.S.J. Suslick, J. Am. Chem. Soc. **102** (1980) 3224.

[59] B.A. Springer, S.G. Sligar, J.S. Olson, and G.N. Phillips, Chem. Rev. **94** (1994) 699.

[60] M. Lim, T.A.A. Jackson, and P.A. Anfinrud, Science **269** (1995) 962.

[61] A. Ghosh, Acc. Chem. Res. **38** (2005) 943.

[62] L. Stryer, *Biochemistry,* ed. 4th, Freeman, New York (1995).

[63] C.K. Bagdassarian, V.L. Schramm, and S.D. Schwartz, J. Am. Chem. Soc. **118** (1996) 8825.

[64] A.K. Bhattacharjee, J. Mol. Struct: Theochem. **529** (2000) 193.